High Aspect Ratio Carbon-based Nanocomposites (HARCANA)

www.HARCANA.eu

HARCANA was organised in a number of work packages dealing with the production and functionalisation of carbon nanoparticles (mainly CNT), and work packages dealing with the preparation of membranes, bulk materials, and foams.

Work Package 3: Production of Carbon-Based Nanoparticles

The production and purification of MWCNT could successfully scaled-up. Furthermore in addition to materials like MWCNT, MWCNT-K (both as synthesized and purified), oxidized MWCNT (MWCNT-COOH and MWCNT-OH) and various graphites, a scale-up of an aromatic amine functionalized MWCNT (MWCNT-NH$_2$) and their dispersion techniques were developed. Master batches could be prepared for various matrix systems.

Work Package 4: Functionalization of Carbon-based Nanoparticles

The preparation of specifically functionalized CNPs and of masterbatches of CNPs with polymers of interest for dispersion in matrices used in WP5, WP6, WP7, WP9 and/or WP10

have been prepared in the frame of WP4. Functionalized CNPs and CNPs masterbatches have been prepared using one of the following methods :

1. Functionalization of CNTs by non covalent approach

Non covalent functionalization of CNTs was carried out by using pyrene-POSS hybrid as a dispersant (Fig. 4.1). The prepared dispersant molecules improve the dispersion of CNTs in organic solvents like tetrahydrofuran, toluene, chloroform and hexane. The functionalized
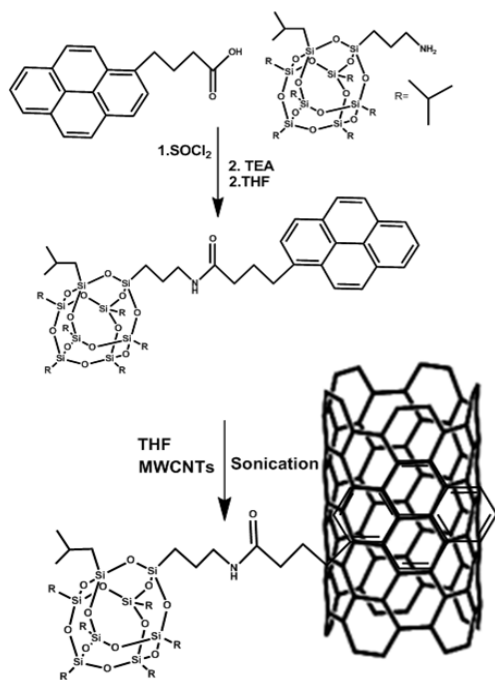

Figure 4.1: Schematic representation of non covalent functionalization of CNTs by pyrene-POSS

CNTs were used to fabricate conductive poly(dimethylsiloxane) nanocomposite membranes for electrostatic discharge (ESD) applications (WP5). It was a challenge to uniformly disperse non functionalized CNTs in a thin PDMS selective layer because of indispersibility of unmodified CNTs in non polar solvents like hexane and toluene. However, Pyrene-POSS hybrid provided the way to disperse CNTs in PDMS nanocomposite membranes with the advantage of well preserved tubular CNTs structure which in turn conserves the electrical properties of CNTs.

2. Specific CNPs functionalization :

Silanol groups have been grafted onto the CNTs surface by a two step process; first the oxidation of the surface (Fig. 4.2a) followed by the inclusion of the silanol groups (Fig. 4.2b). The modified CNPs were fully characterised confirming the presence of silanol groups on the CNPs surface. The dispersion of Si-CNPs in room temperature vulcanised polydimethylsiloxane was performed and the dispersion was evaluated by SEM. CNTs were individually found in the matrix and no agglomerates were observed. The permeability and neural toxicity of these films have been evaluated in the frame of WP5 and WP9, respectively.
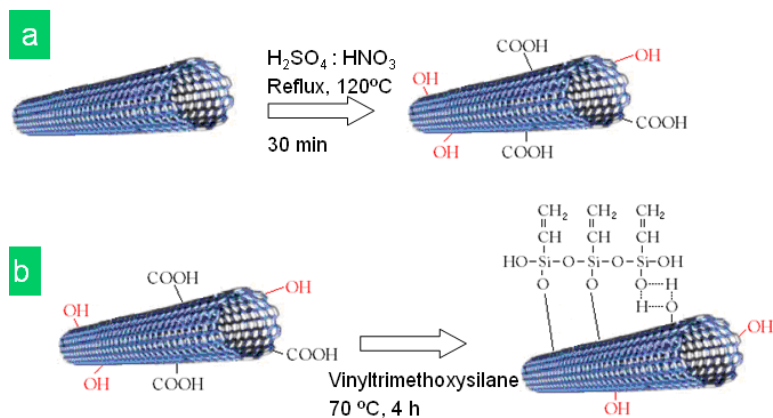
Figure 4.2: *Schematic representation of the silanization procedure.*

The oxidation process (Fig. 4.2a) has also been used to introduce reactive functionalities at the surface of CNTs to be incorporated in rigid polyurethane (PU) foams. Close inspection of the resulting foams by SEM reveals a good dispersion of CNTs throughout the sample, in both the cell walls, and particularly the struts of the cellular structure.

CNTs have also been anchored with various functionalities using the Diels-Alder cycloaddition (Fig. 4.3) with both functionalized furans (dienes) and maleimides (dienophiles), allowing to functionalize nanotubes with, for instance, ATRP initiators (see point 6).
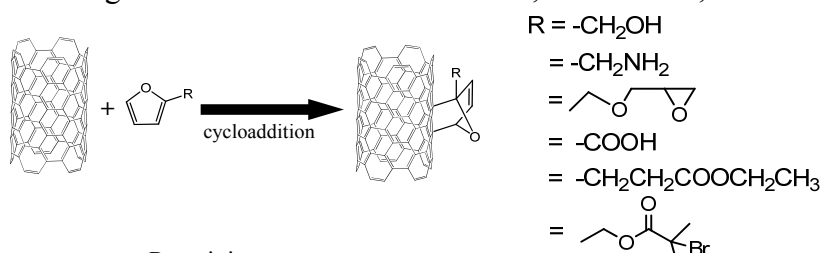

$R = -CH_2OH$

$= -CH_2NH_2$

$= $ (structure)

$= -COOH$

$= -CH_2CH_2COOCH_2CH_3$

$= $ (structure)

Figure 4.3: *Schematic representation of the functionalization of CNTs via Diels-Adler reaction.*

3. Specific physisorption of polymers and block copolymers

In order to master the dispersion state of CNTs in HDPE, one of the prominent matrix studied in WP6 and WP10, a very broad selection of functionalized polyolefins, statistical and block polyolefin-based copolymers have been investigating in order to find a polymeric agent that would allow to control CNTs organization in the semi-crystalline HDPE. Stryrene-*b*-ethylene propylene-*b*-styrene (SEPS) copolymer appeared to be the only matrix able to interact both with HDPE to insure CNTs good dispersion and to prevent specific crystallization of HDPE at the CNT surface, allowing both sufficient CNTs dispersion while not preventing some CNT-CNT connection to occur, necessary for electrical conductivity of the final material to occur at relatively low CNT concentration. The masterbatches were prepared either in melt or in solution.

In another approach used to improve CNTs dispersion in polymers, CNTs were coated with triblock copolymers via physical interaction using a selective solvent approach (Fig. 4.4).

Poly(styrene-*b*-butadiene-*b*-methyl methacrylate) block copolymers (SBM) were used to obtain carbon nanotube masterbatches. In acetone, the polystyrene (PS) and polybutadiene (PB) blocks are in bad solvent while the poly(methyl methacrylate) (PMMA) is in good

solvent. Consequently, the PS and PB blocks are shrunk and localized on the carbon nanotubes surfaces due to solvophobic effects and Van der Waals interactions while the PMMA block is floating in the medium providing the entropic repulsion between adjacent nanoparticles and is insuring stability of the CNT solution for months. Using this method, 25wt% CNT masterbatches were prepared and successfully tested for improving dispersion of CNTs in PVDF (WP5).
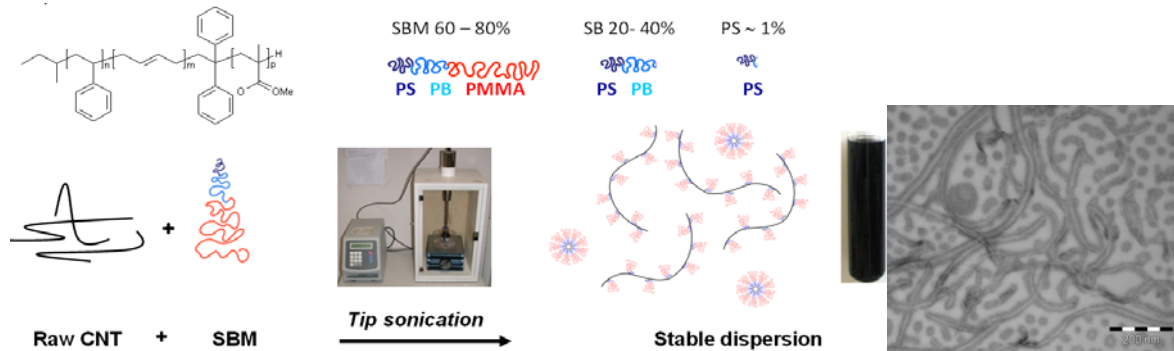

Figure 4.4: *Schematic principle of the stabilization of individual carbon nanotubes with commercial SBM in a selective solvent (acetone) and resulting coated CNTs.*

The originality of these methods is that there is no modification of the CNT' $\pi\pi-$system and therefore it should preserve their intrinsic electrical properties.

4. Masterbatches obtained by in-situ polymerization

In order to improve dispersion of CNTs in PS and styrene-acrylonitrile copolymer (SAN), PS or PMMA (miscible with SAN), masterbatches with high CNTs content (~15 wt%) were prepared by an innovative free radical precipitation polymerization. During its formation, the polymer precipitates entrapping all the CNTs (Fig. 4.5a) as individual nanoobjects (Fig. 4.5b). This method for masterbatch preparation gains advantages over masterbatches prepared by melt blending that does not insure good CNTs dispersion in these matrices and over solution polymerization that would require large amount of solvents for nanocomposite recovery (patent pending). Rheological measurements have confirmed the high efficiency of these masterbatches to improve the dispersion within PS and SAN matrices used in WP6 and WP7.
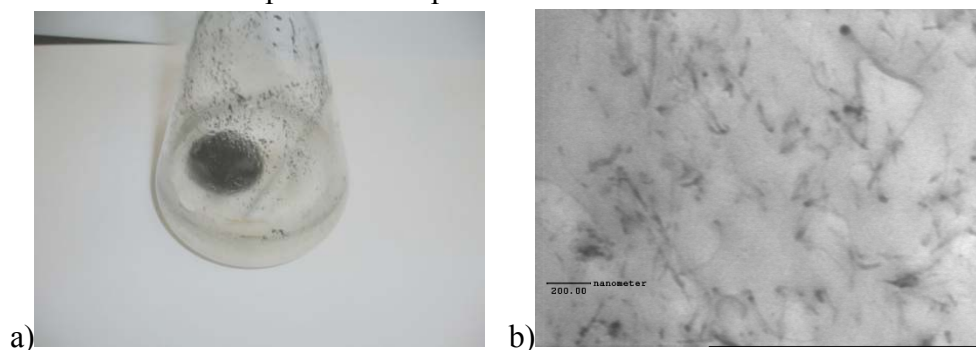

Figure 4.5: *a) Picture of a CNT/PMMA masterbatch at the end of the precipitation polymerization and b) TEM micrographs of a 2wt% CNT/PMMA prepared by precipitation polymerization.*

Mini-emulsion polymerization was another polymerization technique that was successfully used to prepare CNTs/polymer masterbatches and nanocomposites (Fig. 4.6) based on

polyacrylonitrile (PAN), PS, PMMA and SAN polymers used in WP5, 6 and 7. When CNTs are introduced in the formulation for mini-emulsion polymerization, CNTs are partly decorated with polymer chains, improving CNT dispersion in the polymer matrix.
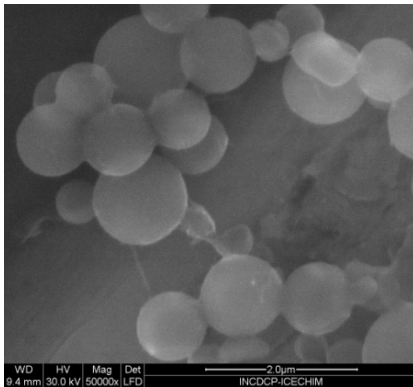

Figure 4.6: *SEM analysis of nanocomposite prepared by mini-emulsion(PS with 1.0% CNT)*

5. *Masterbatches by "grafting-to" processes*

"Grafting to" process, i.e., the formation of covalent bonding between polymer chains and CNPs by using polymer chains bearing end-group capable to react with CNPs surface has also been used as a technique to promote better dispersion of CNTs in polymer matrices. Grafting polystyrene chains (to improve dispersion within PS for WP6 and WP7) or PMMA chains (to improve dispersion within SAN for WP6 and WP7 or within PVDF for WP5) by radical reaction using polymers prepared by nitroxide mediated radical polymerization (NMP) has been carried out. As depicted in Fig 4.7, these polymers are end-capped by an alkoxyamine which can generate radicals at high temperature able to form a covalent bond with CNTs. Significant and stable grafting 13.3 wt% PS and 7.4wt% PMMA were obtained by this method and the obtained masterbatches have been tested in the related WPs.
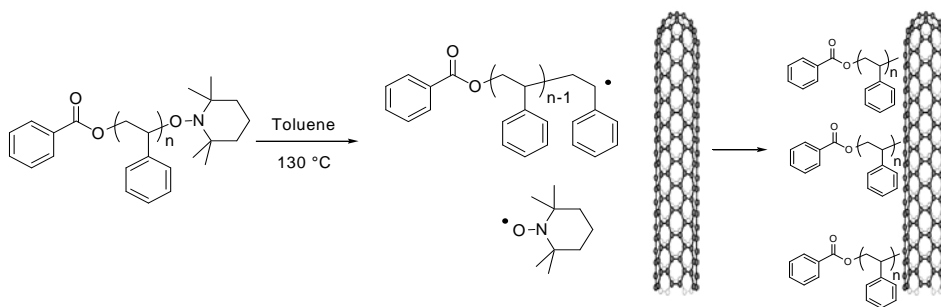

Figure 4.7: *Schematic representation of the grafting of polymer chains end-capped by an alkoxyamine (PS-based system taken as an example).*

The same type of reactive polymer (PMMA end-capped with a nitroxy group) has been used to prepare PMMA-grafted graphene sheet, in a biphasic process where the nitroxy PMMA was dissolved in toluene and covered with a suspension of graphite oxide (GO, prepared by the Hummer's method) in water. Upon heating and addition of a reducing agent (NaBH$_4$), the graphite oxide is reduced and react at the water/toluene interface with radical-ended PMMA activated by heat. A transfer of the PMMA-g-graphene sheets in toluene allows to recover a masterbatch of 15 wt% of PMMA grafted at the surface of conductive graphene sheets. In a simpler, greener process, GO has also been grafted with poly(ethylene glycol) (PEG) chains in water using PEF radicals generated from a commercially available P(PEO-b-diaza)

polyinitiator activated by UV light. A subsequent simple thermal treatment allows to recover conductive PEG-grafted graphene sheets.

6. Masterbatches by "grafting from" processes or polymerization from activated CNTs surfaces

"Grafting from" process is another technique allowing the tethering of polymer chains at the surface of a CNP. In this process, a polymerization initiator is grafted at the CNPs surface and polymer chains grow from it. Macroinitiators for controlled radical polymerization (ATRP) were prepared by immobilizing 2-bromoisobutryl bromide on amine or hydroxyl prefunctionalized CNTs (from WP3) via amidation and esterification reactions, respectively. Alternatively, ATRP initators were also grafted at the surface of pure CNTs using Diels-Alder reaction (see point 2). Grafting of PS and PMMA has been carried out from initiator-modified CNTs in solution using anisole as solvent (Fig. 4.8).
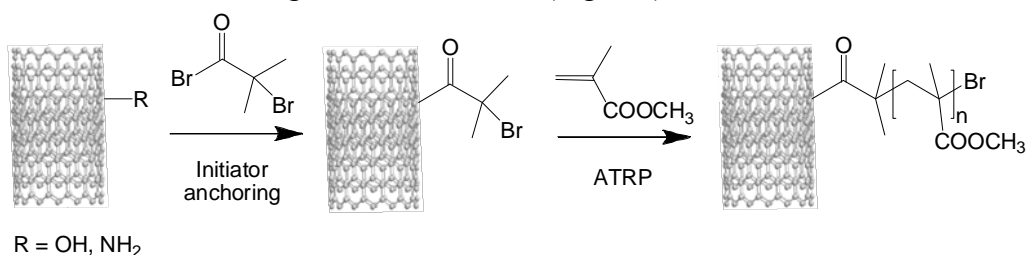

R = OH, NH$_2$

Figure 4.8: *Scheme of initiator anchoring on amine or hydroxyl prefunctionalized MWCNTs and further grafting polymerization of methyl methacrylate.*

The preparation of CNTs anchored with ATRP initiator has been up-scaled up to 10.8g of CNTs treated at once. The up-scaling process was found to slightly decrease the quantity of anchored initiator. When the "grafting from" method is up-scaled (> 500 mg), the quantity of polymer that is actually grafted on the CNTs is decreased. The weight% of grafted polymer remains however quite high (80wt% and 50 wt% for PMMA and PS respectively) compared to results obtained with the "grafting to" method (< 25 wt%). All the dispersions of polymer grafted CNTs in THF were stable for weeks. PMMA grafted CNTs were dispersed in PVDF matrix material for casting membranes for WP5.

Another process, i.e., Ethylene Polymerization Filling Technique (PFT) was attempted to anchor HDPE chains onto the surface of CNT and carbon nanofibres (CNFs). It consists in polymerizing ethylene from the surface of CNTs (or CNFs) by previously depositing methylaluminoxane (as co-catalyst) and a zirconocene catalyst at the surface then polymerizing ethylene in suspension from these CNTs (or CNFs) acting as catalyst support. This process leads to the production of a HDPE-based masterbatches (Fig 4.9).
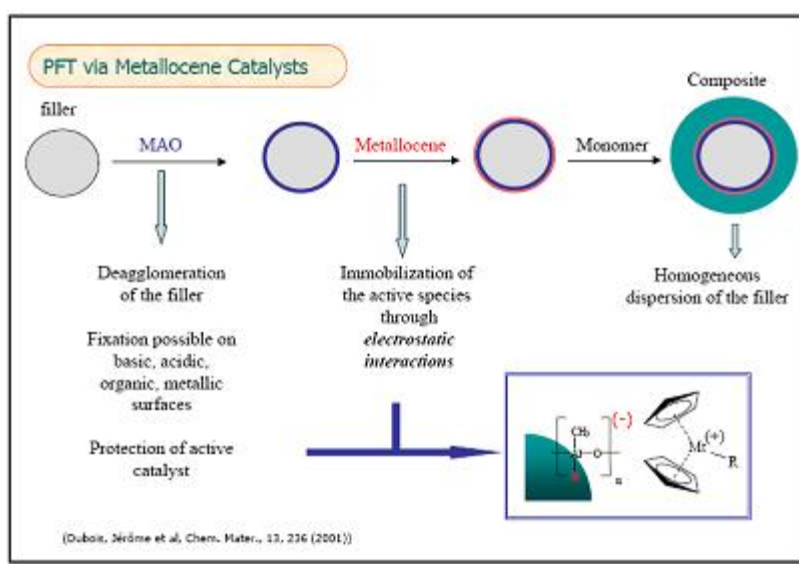
Figure 4.9: *Schematic representation of PFT*

Work Package 5: Thin Film Polymer-CNP-composites

The aim of this work package was the preparation and characterization of novel thin film nanocomposites membranes. Membranes have proven themselves as promising separation tools due to advantages offered by their high stability, efficiency, low energy requirement and ease to process. Membranes with good thermal and mechanical stability combined with good solvent resistance are important for industrial processes. The growing interest in this area led to development of inorganic and polymeric membranes. Generally, inorganic membranes can provide the desired material properties for different separation processes. However, their performance and higher cost compared to polymeric membranes may become a hurdle in industrial applications.

Polymeric nanocomposite membranes based on CNPs from WP3 and WP4 were fabricated. Besides commercial polymers also various families of polymers, useful for the preparation of membranes for specific applications, were prepared. The different thin films were characterized in terms of electrical conductivity and permittivity, thermal and mechanical properties (including rheological), permeability and selectivity besides their morphology (including quantification of the dispersion of CNPs). The aim was to understand the structure property relationships and the special role of CNP, and based on this the design of membranes with superior properties. These membranes were upscaled in WP 10. In addition, some of the thin films of this WP were also delivered to WP 9.

The fabricated nanocomposite membranes were investigated for their use in different areas, from gas separation to ultrafiltration. Promising results were obtained using polyacrylonitrile (PAN) for ultrafiltartion, polymers of intrinsic microporosity for gas seperation (O_2/N_2, CO_2/N_2, and CO_2/CH_4) and conductive PDMS membranes for electrostatic discharge applications.

1. PAN Ultrafiltration Membranes

For ultrafiltration membranes -OH functionalized MWCNTs were blended with PAN to prepare the membranes by a phase inversion process. Different concentrations of MWCNTs were used in PAN, i.e. 0.5, 1 and 2 wt%. The water flux of the membranes increased by 63% at 0.5 wt% loading of MWCNTs compared to neat PAN membranes (Figure 1). The water

flux decreased upon further increase in the concentration of MWCNTs, but at 2 wt% loading it was still higher compared to pure PAN membranes. The surface hydrophilicity of the membranes was enhanced upon the addition of MWCNTs, as observed by contact angle measurements. The increased hydrophilicity might have an impact on the improved water flux and can also have a positive effect on membrane fouling. All the membranes showed a molecular weight cut off of approximately 50 kg/mol (Figure 1). Surface pore size analysis was done by scanning electron microscopy and showed no significant difference in the mean pore size of the nanocomposite membranes compared to the neat membranes. The cross section morphology was influenced by the introduction of MWCNTs where less but enlarged macrovoids were observed, particularly prominent at a loading of 2 wt% MWCNTs. The membranes containing 2 wt% MWCNTs showed 36% improvement in resistance against compaction compared to neat membranes. Furthermore, the tensile strength of the membranes at 2 wt% MWCNTs loading increased over 97% compared to neat ones.
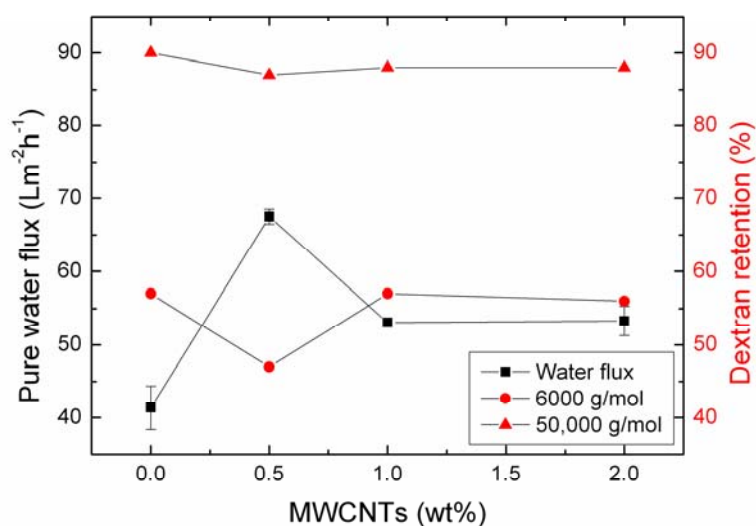

Figure 5.1: *Water flux (left) and retention of 330 ppm solution of dextrans (right) of PAN nanocomposite membranes with different loading of MWCNTs.*

2. Polymers of Intrinsic Microporosity
A novel class of high free volume polymeric microporous material was discovered by Budd, McKeown et al., termed as "polymers of intrinsic microporosity" (PIMs).
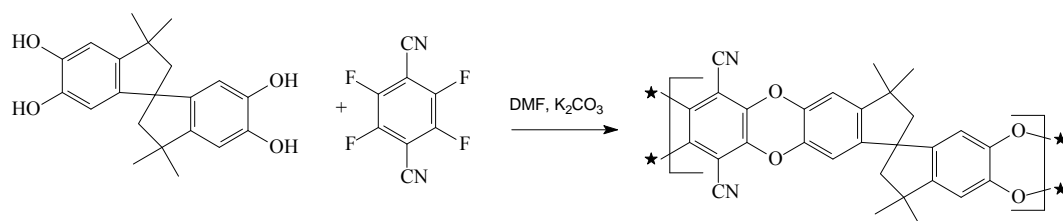

Figure 5.2: *Synthesis of PIM-1 from 5,5´,6,6´-Tetrahydroxy-3,3,3´3´- tetramethyl-1,1´-spirobisindane and 1,4-Dicyanotetrafluorobenzene.*

If the molecular structure of a polymer is highly rigid so that the space efficient packing in the solid state is prohibited, intrinsic microporosity can arise which may create high free volume. Among the polymers having this novel characteristic feature, PIM-1, containing the contorted spirobisindane unit, has so far been the most attractive choice, due to the relative ease of synthesizing polymers with high molecular weight. Moreover, PIM-1 offers the combination

of outstanding permeability with moderate selectivity, especially for O_2/N_2 and CO_2/CH_4 pairs, which shows the upper bound trade-off introduced by Robeson. However, the biggest challenge of PIM-1 to find a practical use in gas separation technology has been the significant loss of permeability in long-term measurements.

Several studies have been reported to solve this problem as well as to further improve the permeability and selectivity of pristine PIM-1 by modifying the molecular design without success.

The gas transport behavior of mixed matrix membranes (MMM) prepared from multi-walled carbon nanotubes (MWCNTs) dispersed within a PIM-1 matrix was studied. The MWCNTs were chemically functionalized with polyethylene glycol (PEG) for a better dispersion in the polymer matrix.

The gas permeances of the derived MMM are increased ~50% without sacrificing selectivity at 2 wt% PEG-MWCNTs loading. The PEG groups on MWCNTs have strong interaction with CO_2 which increases the solubility of polar gas and limit the solubility of non-polar gas, which is advantageous for CO_2/N_2 selectivity. The addition of PEG-MWCNTs inside the polymer matrix also improved the long term gas transport stability of MMM in comparison with PIM-1. The high permeance, selectivity, and long term stability of fabricated MMM suggest that the reported approach can be utilized in practical gas separation technology.
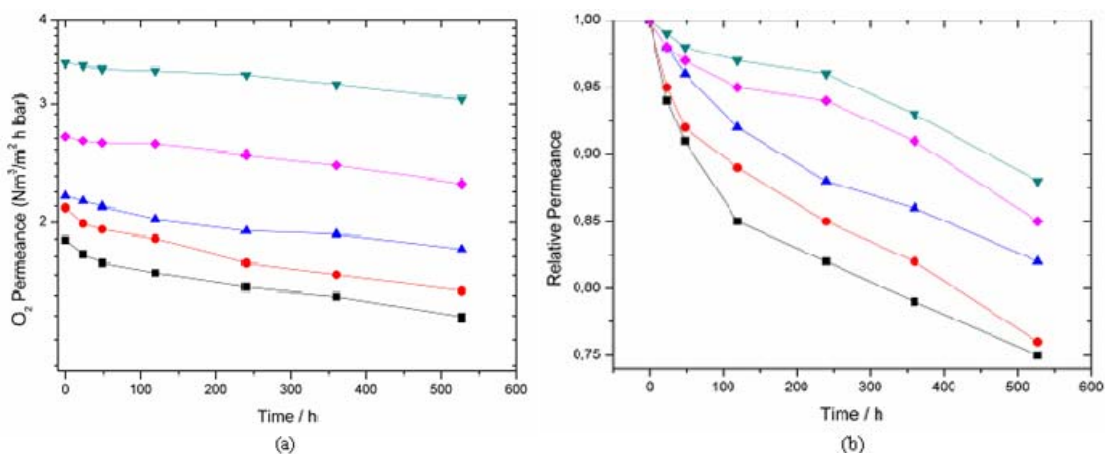

Figure 5.3: *Long term stability of PIM-1; PIM-1 MMM incorporated with f-MWCNTs measured as (a) O_2 permeance; (b) relative permeance.((■) PIM-1, (●) 0.5 wt% MMM ,(▲)1 wt% MMM, (▼)2 wt%MMM), (♦) 3 wt% MMM, Temperature: 27 °C; Feed pressure: 2 bar*

3. PDMS Nanocomposite Membranes

In order to avoid electrostatic charges in membranes, electrical conductivity was introduced by blending the membrane matrix with MWCNTs. It was a challenge to uniformly disperse non-functionalized MWCNTs in a thin PDMS selective layer. Non covalent functionalization was carried out by pyrene-POSS dispersant to improve the dispersibility of MWCNTs in toluene and hence in PDMS selective layer. Non covalent functionalization is a defect free functionalization method and it led to well dispersed (Figure 5.4) and highly conductive PDMS membranes (Figure 5.5). The conductive membranes, during their application in plastic made membrane modules, can provide the opportunity to neutralize the electrostatic charges and hence may provide a safer separation of hydrocarbons. Due to the good dispersion of MWCNTs with the method developed by HZG was it possible to produce conductive membranes.
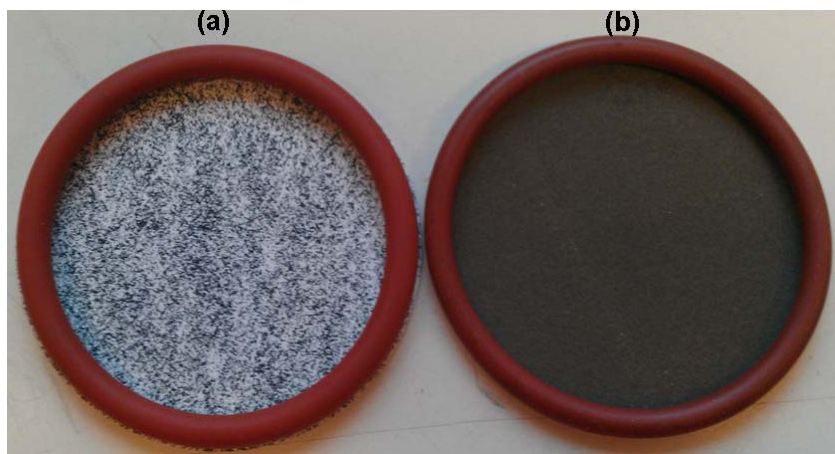
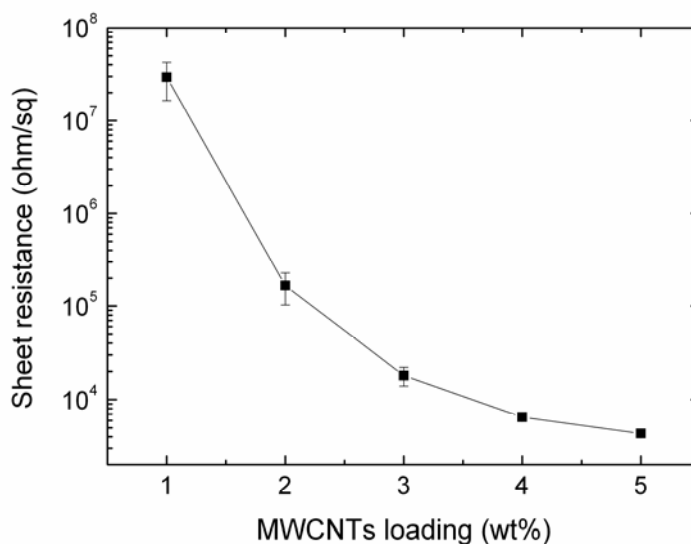***Figure 5.4:*** *Digital photograph of PDMS membranes (a) 6 wt% purified MWCNTs and (b) 3 wt% PP-MWCNTs*

Figure 5.5: *Electrical sheet resistance of PDMS membranes as a function of pyrene-POSS modified MWCNTs loading.*

Work Package 6: Bulk Polymer-CNP-Composites

WP6 focused mainly on the manufacture of nanocomposites of (co)polymers and polymeric blends where the CNP is selectively localised in one phase or at the interface. More specifically, the aim of this WP was to better understand the relationships between the morphology with a special focus on the localisation of the CNP and the resulting properties of the nanocomposites. The strategy adopted in this WP was to manufacture bulk nanocomposites based on masterbatches prepared in WP4. Several types of systems were studied and one system (HDPE based composites) was more specifically dedicated to WP10 application dealing with fuel tank materials. 2 patent applications and more than 14 peer reviewed papers are issued from WP6 studies. Main scientific achievements of WP6 can be summarized as follows:

-*For semi-crystalline polymers*, the research realized in WP6 highlights a simple way to tune HDPE nucleation using an elastomer which exhibit good affinities with CNT and partial compatibility with HDPE. This polymeric modifier allows to decrease the size of insulating HDPE crystals generated from CNT surface and it also promotes CNT dispersion within HDPE leading to a substantial improvement of HDPE composite electrical properties as well as their stabilization. In addition, due to its elastomeric nature, the impact strength of the composite is maintained (Figure 6.1). These compositions have been the subject of a patent in the frame of HARCANA project.
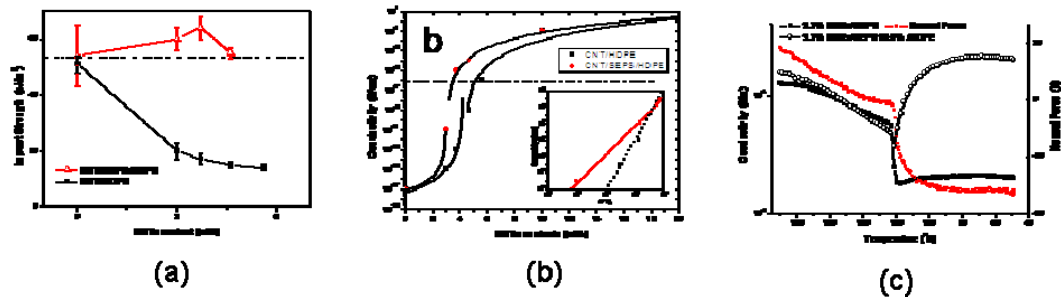

(a)   **(b)**   **(c)**

Figure 6.1: *Effect of polymeric modifier (SEPS) on HDPE/CNT composite properties: a) impact strength b) electrical conductivity c) stability of electrical properties*

-*For amorphous homo and random copolymers*, 2 types of systems must be distinguished and stressed from WP6 studies.

1) For thermoplastics, 2 techniques gave main results of interest. First, CNT prepared by polymerization precipitation which consists in entrapping CNT during polymerization of PS or PMMA monomers in the presence of CNT in a bad solvent of the polymer. Interestingly enough, this technique was the subject of a patent application in the frame of HARCANA project.

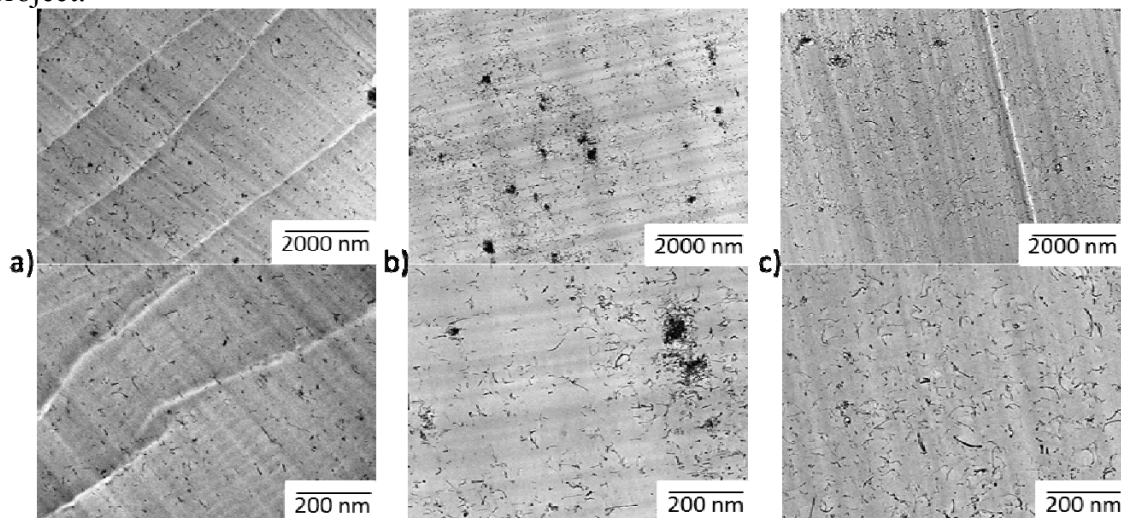***Figure 6.2****: Comparison of CNT dispersion within PMMA matrix following different preparation processes a) melt-mixing, b) co-precipitation and c) precipitation polymerization*

Second, use of polymer functionalized CNT. Both techniques allow a significant improvement of CNT dispersion within SAN, PMMA and PS matrices leading to a substantial improvement of electrical properties of the composites. (Figures 6.2 and 6.3)
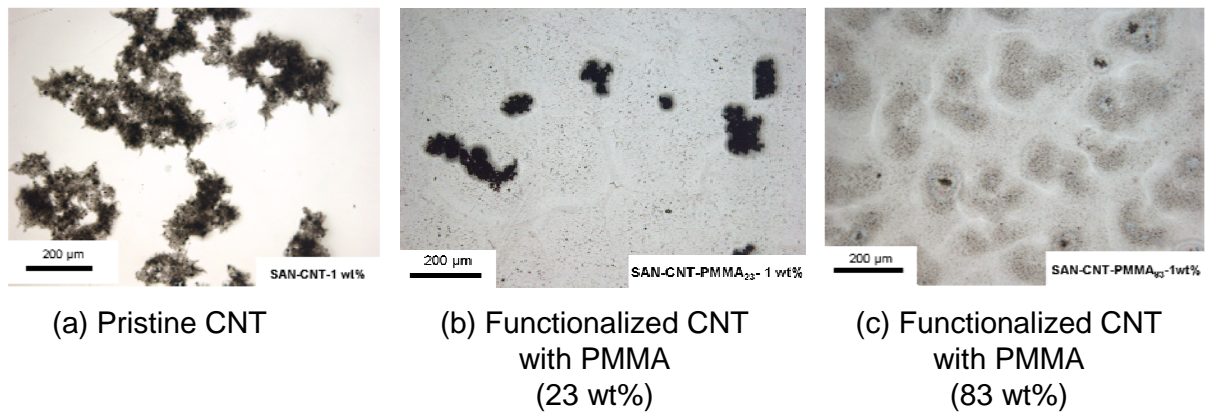
(a) Pristine CNT

(b) Functionalized CNT
with PMMA
(23 wt%)

(c) Functionalized CNT
with PMMA
(83 wt%)

Figure 6.3: Effect of CNT functionalization on CNT dispersion within SAN matrix

2) For elastomers, preparation conditions were found to be critical parameters for the control of the CNT and CNS dispersion within PDMS and EPDM matrices. The best dispersed systems result in improved electrical properties as well as enhanced mechanical properties.

-For (co-continuous) polymer blends, 2 main systems appear of interest and were deeply investigated in the frame of WP6.

1) SAN/PPE systems: the research highlights that the key parameters to tune CNT confinement are the nature and the molecular weight of the polymer grafted from the surface of CNT. For instance, CNT dispersion is uneasy within PPE in the melt due to PPE high processing temperature. Due to the PS compatibility with PPE, CNT functionalized with PS can be selectively driven to PPE phase in the melt (Figure 6.4).
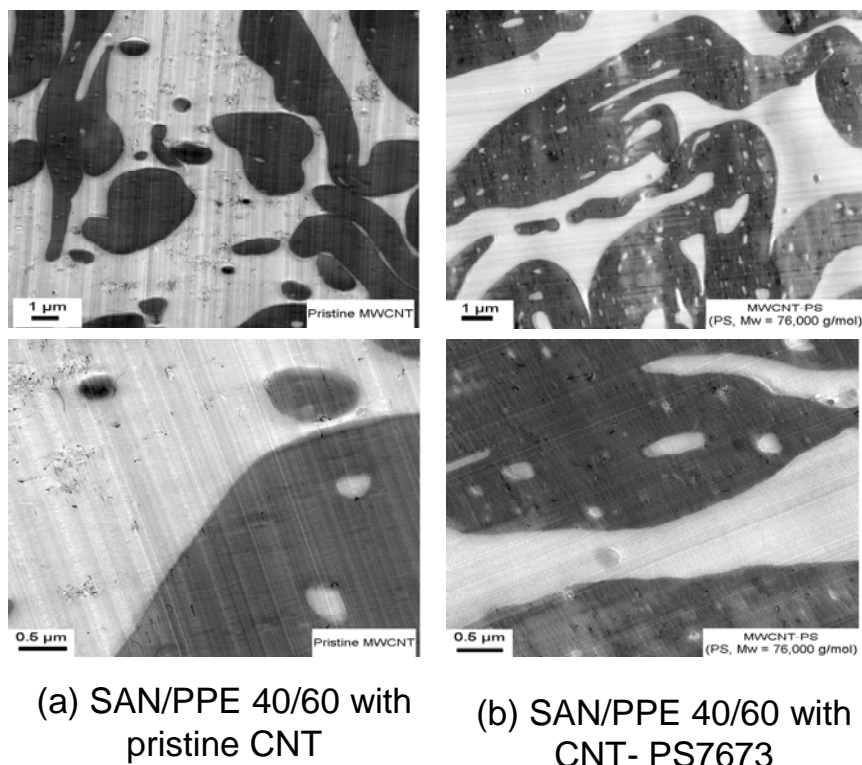

(a) SAN/PPE 40/60 with
pristine CNT

(b) SAN/PPE 40/60 with
CNT- PS7673

Figure 6.4: Effect of CNT functionalization on CNT confinement within SAN/PPE matrix

2) reactive PE/PA blends: 3 different approaches can be stressed.
The first approach confirms the possibility to confine CNT by tuning polymer-CNT interactions using CNT with different surface functionalization. The nature and the molecular weight of the polymer grafted (covalently or not) on the surface of the CNT appear to be the critical parameters to drive CNT.
The second approach focuses on co-continous nanostructured reactive PE/PA systems. PA nanodomains were found to be bridged by CNT allowing the formation of a double interconnected network which lead to significant increase of thermomechanical properties of the system. For lower amounts of PA, PA nanodomains become micellar and they were found to solder CNT into a continuous network leading to solvent resistance of the system as well as enhancement of its thermomechanical behaviour (Figure 6.5).

The third approach highlights the possibility to obtain nanostructured nanocomposites with a fine dispersion of CNT using a masterbatch of reactive polymer with CNT.

-*For block copolymer systems*, mainly 2 types of systems were found of interest.
1) Results stressed that the morphology of styrene-butadiene block copolymer/CNT films is mainly influenced by the PS chain grafted from CNT surface. When CNT are grafted with higher molecular weight and PS grafted content is important, CNT were found to template the lamellar morphology of the block copolymer.

2) Results highlight that by fixing the processing procedure, it is possible to obtain poly(styrene-block-butadiene-block-methyl methacrylate)/CNT composites with reproducible microstructure and properties.
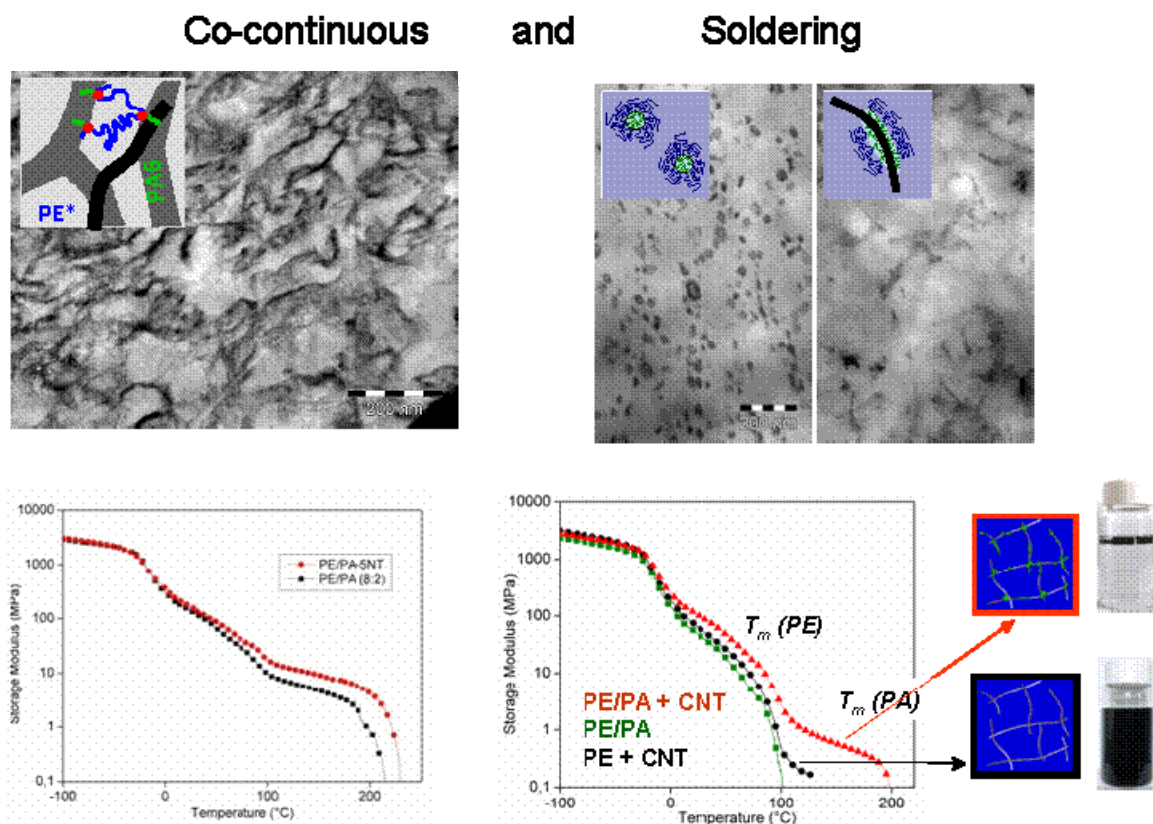

Figure 6.5: *Morphology and properties of reactive PE/PA composites: a new range of thermo-mechanical properties appear between 100°C and 200°C*

Work Package 7: Foams of polymer-CNP-composites

The purpose of WP7 was to develop novel routes for the production of polymer-based nanocomposite foams (Figure 7.1). The two objectives of the work done on polymer foams are the development of new lightweight and efficient electromagnetic interference (EMI) shielding materials and optimised neuron foam scaffolds.
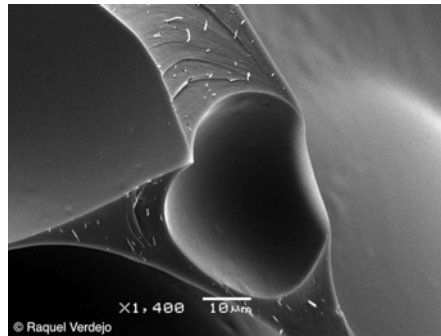

Figure 7.1. *Carbon nanotubes reinforced closed-cell PU nanocomposite foams*

Both thermoplastic and thermoset polymers were foamed using two manufacturing processes: a) supercritical CO_2 and b) batch techniques. The project subsequently studied the effects of CNPs from WP3 and 4 on the processing and the foams' porous structure and their physical and chemical properties. Special attention was paid on the development of rigid Polyurethane foams for EMI shielding. The main scientific achievements of WP7 are summarised in terms of the processing protocol:

1. supercritical CO_2

The preparation of polymer/CNT foams using the supercritical CO_2 technology have been concentrated on the foaming of four different polymer matrices poly(methyl methacrylate) (PMMA), poly(styrene-*co*-acrylonitrile) (SAN), thermoplastic polyurethane (TPU) and a polypropylene with low crystallinity (PP)) using two different foaming protocols: the one-step process and the two-steps foaming process.

The introduction of MWCNTs in the polymers modified the foaming process (by increasing the melt strength of the material) and the microscopic morphology of the foams (MWCNTs acting as nucleating agents, leading to more numerous smaller cells).

The EMI results clearly showed that the addition of CNTs allows reducing the quantity of radiation transmitted, by absorbing up to 50 % of the incident energy at 10 Hz. The best absorption/reflectivity ratios were clearly obtained by the foams with the highest volume expansion (PMMA and PP), which confirm the advantage to prepare polymer/CNTs for the reduction of electromagnetic interference. The absorption coefficient significantly increases with the frequency to reach value superior to 95 % between 30 and 40 GHz. These samples are then very interesting for all applications dealing with this kind of frequencies. We have not observed any improvement (nor significant degradation) of the mechanical properties of the tested foams and an interesting flame retardant effect has been qualitatively observed for TPU foams containing 1wt% of MWNTs.

2. batch techniques

This processing technique was used to develop free-rise polyurethane (PU) foams. Two sets of PU foams were prepared: open cell flexible PU and close cell rigid PU foams. These foams are generally obtained from the simultaneous reaction of a polyisocyanate with a polyol

matrix and water. These reactions generally result in a segmented block copoly(urethane-urea). Hence, PU foams present a hierarchical structure: the matrix phase-separated block copolymer morphology at the nanoscale and the cellular structure at the microscale. The inclusion of MWCNTs and functionalised-MWCNTs was shown to affect mainly the matrix microstructure (Figure 7.2) and not the cellular structure. The presence of the nanoparticles decreased the rate and extent of the polymerisation reaction. The study also revealed the existence of a relationship between the kinetics of polymerization and the kinetics of phase separation in PU nanocomposite foams. The studies have been published in two peer-reviewed articles.
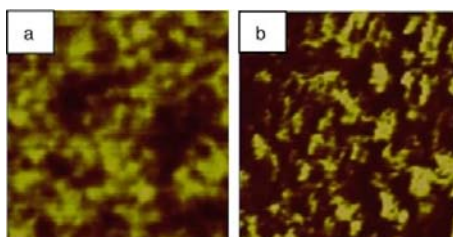

Figure 7.2. Tapping mode AFM phase images of flexible PU foam and its nanocomposite. Images are displayed at a total phase scale of 25° and the scan width is 500 nm. a) Neat and b) MWCNTs samples, where the light colour are urea hard domains and the dark areas are the soft segment domains.

The thermal stability of both flexible and rigid PU foams was greatly improved by the presence of CNPs, with an increase of up to 40 °C for flexible PU foams filled with functionalised graphene sheets. Additionally, flexible PU foams were mechanically reinforced by the presence of CNPs. The presence of CNPs increases the values of the specific EMI shielding effectiveness. While the average value for neat rigid PU foam was approximately 4 $dB·cm^3·g^{-1}$, the inclusion of 0.35 wt.-% of MWCNTs at 12 GHz was around 38.7 $dB·cm^3·g^{-1}$. PEG-g-MWCNTs raised even further the conductivity of the samples to a target value of 0.4 S/m at a filler loading of only 0.35 wt.-%. Although the properties were improved by using polyol functionalised MWCNTs, the properties did not reach the envisioned values of conductivities and low density. However, target conductivities were achieved at a higher foam density.

Work Package 8: Modeling of Polymer-CNP Composites

An essential aspect of the HARCANA research is the control of the dispersion of carbon-based anisotropic nanoparticles (CNPs) in polymer matrices targeted for specific applications in membranes, foams and the automotive sector. A key parameter impacting dispersion is the strength of the **interactions at the polymer/carbon interface**. Therefore, understanding the structure and energetics of those interfaces appears as a powerful means for determining which polymer material is most likely to act as an effective matrix for the carbon particles. This forms the first part of the research conducted in this WP. Also, proper dispersion of CNP in polymer matrices fixes the electrical conductivity of the composite, which is the key parameter involved in **the theoretical prediction of EMI and ESD performances of Polymer-CNP nanocomposites**, which forms the second objective of WP8.

Molecular modeling can provide a major contribution to understanding CNP-polymer interactions. Here the theoretical approach was used to investigate model systems for the interfaces, both from the structural standpoint (i.e., the molecular-scale organization of the

polymer chains at the surface of the carbon particle) and the energetic standpoint (i.e., the nature and intensity of the intermolecular interactions between the components).

In practice, the model systems under consideration were defect-free carbon nanotubes (CNTs) interacting first with a single chain of prototypical polymers selected among the following set: polycaprolactone (PCL), polyamide-6 (PA6), polystyrene (PS), polyethylene (PE), polyethylenepropylene (EP), polyisobutylene (PIB), polyethyleneoxide (PEO) and poly(styrene-ethylene/propylene-styrene) block copolymer (SEPS). A variety of structural units (polar vs. non-polar; aliphatic vs. aromatic) and chain architectures (homopolymers vs. random/block copolymers) has thus been considered. The typical modeling started with Molecular Dynamics simulations of one polymer chain in contact with the nanotube in different chemical environment (vacuum, liquid or pseudomelt, i.e., when more interacting polymer chains are made interacting with the CNT). The modeling of the polymer-CNT interface focused on the influence of the chemical nature of the polymer repeating units and the polymer tacticity on the strength of the interaction between polymer and the wall of the CNT. Also, the morphology adopted by the polymer chain has been intensively investigated. The results on the model systems investigated can be summarized as follows:

- The meaningful parameters to compare different polymer/nanotube systems are the adhesion energy expressed per unit of polymer/nanotube contact area and the polymer/nanotube contact area, which depends of the chemical environment. Remarkably, despite the different morphologies of the adsorbed polymers, PCL and PA6 have a very similar adhesion energy per unit of contact area. On the contrary, the strength of the interactions with the nanotube is twice as small for PS. These trends are coherent with the experimental observations: PCL and PA6 are known to form good-quality dispersions with nanotubes, whereas the CNTs very poorly disperse in polystyrene.

- PCL, PE and PA6 chains fold on the nanotube wall in a regular structure, with parallel linear segments that are slightly tilted with respect the axis of the nanotube. PS, depending on the tacticity, can fold like PE or adopt a linear conformation.

- The quality of the polymer adsorption and polymer morphology on the nanotube can depend on the environment, i.e., on the conformation of the polymer chain before adsorption on the CNT surface. In the case of the adsorption of PA6 on CNT in vacuum, i.e., in an ideal bad environment for the polymer, the PA6 chain remains coiled when adsorbed on the nanotube and does not strongly interact with the surface. The reason for this behavior lies in the presence of strong H-bonding within the polymer coil, between the amide groups of PA6. In a good environment for PA6, e.g., in formic acid, the PA6 chain uncoils and completely adsorbs on the nanotube surface, forming a regular, folded (or lamellae) conformation. This is mainly due to the fact that formic acid can promote competitive H-bonds with the amide groups in the polymer, allowing the coiled polymer chain to swell easily when interacting with the nanotube, and to rearrange on the surface towards a more organized situation. With the polymer completely adsorbed, the strength of the polymer/CNT interaction is higher than for adsorption taking place in vacuum. For other polymers, such as PCL, PE and PS the results are less affected by changing the nature of the surrounding medium

- The presence of chemical defects, such as -OH, NH_2 and -COOH groups, can dramatically affect the morphology of the polymer chain at the interface, especially when specific interactions are present between the defects and the polymer. In the case of PCL interacting with a –COOH functionalized nanotube, the regular lamellae structure observed on a pristine nanotube is strongly distorted, and translates into a weaker interaction between the polymer chains and the CNT.

As molecular dynamics simulations cannot explicitly account for electronic effects, such polarization at the interface, polarization effects between the polymer chains with and without polar groups (PE, PEO, PCL and PA6) and the nanotube have been investigated by means of

periodic quantum-mechanical Density Functional Theory. Those calculations show that the polarization effects are negligible in the case of PE/CNT interfaces, while they become increasingly important with the polarity of the groups in the polymers interacting with the nanotubes. The polarization induced in the nanotube wall when a polymer chain containing polar groups is interacting with the CNT contributes to stabilizing the polymer chain at the interface.

Moving towards mesoscale modeling, multiple polymer chains – CNP interfaces were first investigated, considering five interdigitated polymer chains in contact with a nanotube. The morphological analysis of those PE pseudomelts predicts, in agreement with experimental evidence reported in literature, that the nanotube promotes the formation of PE lamellae radiating (in orthogonal direction) from the nanotube wall. The high adsorption energy of the regular folded chain at the interface indicates that the nanotube acts as a nucleating agent for the PE crystallization.

As atomistic models have to be limited in both size and time scales, compared to the huge number of interactions present in bulk polymer melts and nano-composites materials, a coarse graining technique was then developed and tested. It enables to increase the size and the time scale of the system to model by merging groups of atoms into "super-atoms" called beads, hence reducing the number of interactions to compute.

From the results of the molecular modeling, one can propose general guidelines on the type of polymers that are likely to interact favorably with CNTs, and therefore act as effective matrices for CNT dispersion.

1. Linear polymer chains containing oligomethylene segments (as observed for PE, PEO, PCL and PA6) appear as a favorable structure, probably because those segments can form numerous CH-π interactions with the nanotube surface.

2. In contrast, polymer chains with bulky side groups are expected to interact poorly with the surface. In the case of PS, the phenyl rings are not able to promote efficient π-π interactions with the CNT surface, due to steric constraints. Note however that polymers in which aromatic units are inserted in the main chain would be more prone to interact favorably with CNTs.

3. The presence of polar groups (e.g., ester or amide) along the polymer backbone also seems an important parameter, probably because they induce intrachain intermolecular interactions that favor adsorption in ordered conformations (e.g., lamellae).

On the RF modelling side, models were developed and tested at two different levels: the material properties of the composite, and the design of EMI shielding and absorber topologies. *At the composite level*, the RF parameters of interest are the complex permittivity $\varepsilon_r' = \varepsilon' - j\,\varepsilon''$, or equivalently the dielectric constant (ε') and the conductivity ($\sigma' = -\,\omega\varepsilon_o\,\varepsilon''$) of the nanocomposite. Electrical percolation was modeled according to a power scaling law for the direct-current (DC) conductivity, with values of fitting or scaling parameters dependent on the aspect ratio of the CNP particles, and 2D or 3D dimensionality of the system. Another power law can be established to describe the frequency dependence of this conductivity, depending on the CNP dispersion state: below or above a percolation threshold. Below threshold, the power law describing conductivity versus frequency shows, for each CNP concentration, a linear dependence in double logarithmic scale, over the whole frequency range, while the dielectric constant has moderate values that do not vary with frequency. Above threshold, in the upper range of CNP concentrations, the linear behavior of conductivity is still present in the upper range of the frequency spectrum, while at low frequencies the conductivity shows a nearly constant (or "plateau") behavior versus frequency. The dielectric constant exhibits a decrease from high values to low asymptotic values with an inflexion point situated at the same transition frequency as observed for the conductivity.

Power scaling laws are quite empirical, in the sense that their parameters are fixed/fitted from experimental observations. Another family of models aims at describing electrical interactions between CNP inclusions and hosting matrices, taking into account their orientation, aspect ratio, interdistance and concentration. The equivalent circuit approach was such demonstrated to be a powerful tool for explaining the frequency dependent behavior of conductivity and dielectric constant, because it models interactions between CNPs and electromagnetic signals by resistances, inductances and or capacitances. A last powerful modeling approach is based on the effective medium theory. Using averaging techniques, it enables predicting over the whole frequency range the values of the permittivity, or equivalently the dielectric constant and conductivity, whatever the concentration of CNPs, their aspect ratio (sphere, wire or platelet) and orientation (random dispersed or aligned along a particular direction).

Next, the possible correlation between electrical percolation and rheological analysis, further supported by TEM microscopy, was studied. As for the DC conductivity, the increase of storage modulus G' at oscillatory frequency at low frequency towards the plateau is the signature of a rheological percolation, meaning that the motion of some polymer chains is restricted because of a presence of CNPs network. The rheological behavior of two-phase systems with CNTs mainly confined at the interface between dispersed and continuous phases was successfully predicted using the Palierne formalism.

Finally, using former models for dielectric constant and conductivity of CNP nanocomposites, an efficient transmission line model was tested to predict the three interdependent mechanisms involved in the operation of efficient composite architectures for reduction of Electromagnetic Interferences: reflection, transmission and absorption. As a first design rule, an efficient microwave absorber must combine a low reflection of waves at its interfaces with surrounding air (meaning a low dielectric constant), and a good absorption obtained by high conductive dissipation of power over the slab thickness. Since an increase in conductivity induced by a higher CNP wt loading goes in hand with an increase of dielectric constant, this issue can be solved at a given slab thickness by replacing a single layer of nanocomposite by a multilayer of same overall thickness with successive layers showing increasing CNP concentration. Other promising metamaterial topologies were proposed: electromagnetic bandgap structures, and selective surfaces, controlling the propagation of waves depending either on their frequency or their electromagnetic polarization, thanks to the periodicity, shape and alignment/orientation of conductive inclusions or thin films. Such structures are good candidates for obtaining smart, compact and easily conformable materials for reducing EMI issues.

Work Package 9: Biocompatibility of polymeric-CNP-Composites

The general objective of WP 9 was to test the biocompatibility of carbon-based nanocomposites with neural cells both in cell culture (*in vitro*) and *in vivo*. In particular, the biocompatibility of Multi Wall Carbon Nanotubes (MWCNTs), PVDF membranes, PDMS and PCL foams, and Functionalised Graphene Sheets (FGS), has been studied.

1. Objectives of the in vitro studies
The in vitro experimental aproaches have been used to determine the effects of the materials on the following processess: 1) toxicity or the absence of toxicity to neural cells, 2) proliferation of neural stem cells (NSCs), 3) multipotent differentiation of NSCs to the major cell types of the brain, i.e, neurons, astrocytes and oligodendrocytes, 4) expression of the main transcription factors that regulate the generation of the mentioned cell types, 5) survival of neurons, astrocytes, and oligodendrocytes, 6) morphological maturation of neurons and oligodendrocytes, and 7) synaptic maturation of neurons.

2. Methods of the in vitro studies.

As mentioned above, the large majority of the *in vitro* studies have been performed on NSCs isolated from the olfactory bulb (OB) of adult mice (a region of the brain where active neurogenesis occurs throughout the life of the animal) and only a minority of analyses have been carried out in neurons isolated from another brain region, the hippocampus (a brain region that also maintains active neurogenesis throughout the life of the animal). NSCs are undifferentiated cells that can self-renew and that can give rise to the three major cell types in the brain, namely, neurons, astrocytes and oligodendrocytes. As such, NSCs are of great interest to be used in cell therapy aimed at producing neuroregeneration.

For the large majority of assays, adult olfactory bulb stem cells (aOBSCs) are initially grown as neurospheres; then disaggregated, plated on top of glass coverslips, and fixed at different times with 4% paraformaldehyde (PFA). The cells are then immunostained with specific antibodies or processed for electron microscopy (TEM and SEM). Staining the cells with 4',6-diamidino-2-phenylindole (DAPI$^+$) and immunostaining with specific antibodies followed by observing cell nuclei in a fluorescence microscope and cell counting, have been used to monitor the survival and lack of toxicity of the different CNP composites. To study the influence of FGS on the expression of transcription factors involved in the formation of neural cells, the RNA was extracted from cultured cells, its purity and integrity determined, and this was followed by a reaction catalyzed by a reverse transcriptase to convert mRNA into cDNA. Specific regions of cDNA for each transcript were amplified using the Polymerase Chain Reaction (PCR), and the corresponding bands visualized on agarose gels.

3. Results and Conclusions of the in vitro studies.

3.1. The attachment of the nanotubes to the coverslips and of the cells to the nanotubes is sub-optimal. Better results were obtained with MWCNT-amino than with non-functionalized MWCNT.

3.2. Adult olfactory bulb stem cells (aOBSCs) differentiate into neurons, astrocytes and oligodendrocytes when grown on MWCNTs (purified and aminofunctionalized). However, a safety issue concern arises from the metal catalysts that remain in the MWCNTs which could be toxic for neural cells isolated from both, the olfactory bulb and the hippocampus.

3.3. The information resulting from the experiments performed indicate that the cells could not attach to the PCL and PDMS foams. Thus, the effect of these materials on cell survival, proliferation and differentiation could not be tested in the HARCANA project.

3.4. Adult olfactory bulb stem cells (aOBSCs) generate neurons, astrocytes and oligodendrocytes when seeded on PVDF membranes (standard and MWCNT-modified) suggesting that these materials are biocompatible, non toxic for neural cells. This should be ultimately corroborated by performing cell death assays.

3.5. The same numbers of neurons were detected in all the conditions (Control PLO/F, PVDF, and MWCNT-PVDF). Neurons differentiating on MWCNT-PVDF films tend to grow fewer but longer neurite branches than those growing on standard PVDF membranes.

3.6. Standard PVDF membranes appear to be superior to the modified ones for oligodendrocyte survival. However, the morphological maturation of oligodendrocytes could be favoured when aOBSCs are differentiating on the modified membranes.

3.7. Our results confirm that aOBSCs can proliferate and form neurospheres in the presence of FGS. However, the size and shape of these neurospheres appear sub-optimal compared to controls.

3.8. Similar proportions of each cell type (neurons, astrocytes and oligodendrocytes) were observed in control conditions compared to FGS, indicating that graphene is a permissive substrate which supports the multipotent capacity of aOBSCs to differentiate into the major brain cell types.

3.9. We have determined: a) that the resistivity of FGS is 3.7x10-4 Ω.m; b) using AFM we have confirmed that FGS form a layer of 1-3 nm after drop-cast onto PEI-coated coverslips; and c) using TEM we have observed that graphene is in close contact with the cells plated on FGS-treated coverslips.

3.10. We have studied the effects of FGS on the morphological and synaptic maturation of aOBSC-derived neurons in cell culture and on freshly isolated neurons. The density of synaptic boutons (as determined by immunostaining with an anti-synaptophysin antibody) and the bouton perimeter suggest that graphene is a permissive substrate for synaptic maturation. The effects of FGS at both EM and electrophysiological level are currently being analysed.

3.11. Our gene expression studies indicate that FGS supports the expression of key transcription factors which regulate the formation of neurons, astrocytes and oligodendrocytes from aOBSCs.

4. Objectives of the in vivo studies
The *in vivo* approaches have been used only with the selected material from the *in vitro* studies, in particular, with FGS as we found this material to be biocompatible, non-toxic to neural cells. We have analysed the effect of FGS on the following processess: 1) toxicity to neural cells, 2) inflammation, 3) cell death and survival of neurons and astrocytes, 4) neuronal generation from dividing neural stem and progenitor cells, 5) morphological and synaptic maturation of newly generated neurons.

5. Methods of the in vivo studies.
FGS at a concentration of 0.004 μg/μl was injected together with a vector expressing the enhanced green fluorescent protein (EGFP) in the subependymal zone of the adult olfactory bulb following our protocols with some modifications. This vector allows visualization of newly formed neuronal (Fig. 9.1) and glia from dividing cells. The mice were anesthetized one and two weeks post-injection, and then perfused transcardially with 0.9% NaCl and 4% PFA. Their brains were postfixed, embedded in 3% agarose and serial coronal vibratome sections were obtained. Sections containing the OB were collected and immunostained with specific antibodies or processed for EM. All animal care and handling was carried out in accordance with European Union guidelines and was approved by the Comisión de Bioética (Ethical Committee certificate issued on July 6th 2007). All efforts were made to ameliorate the suffering of the animals.

6. Results and Conclusions of the in vivo studies.
6.1. The presence of FGS in the tissue has been detected by EM.

6.2. Immunohistochemistry with antibodies against doublecortin (DCX, a marker of immature neurons), NeuN (a marker of mature neurons), GFAP (an astrocyte marker) and IBA-1 (a microglial marker indicative of inflammation) shows no deleterious effects of FGS on neurons and astrocytes.

6.3. In addition, the results show that new neurons can be generated in the adult mouse OB in the presence of FGS.

6.4. We have seen no inflammation response caused by the injection of FGS.

6.5. All these findings suggest that graphene could be biocompatible with brain cells in vivo. However, more experiments injecting EGFP-expressing vectors and aOBSCs in combination with FGS, are in progress to support these conclusions.
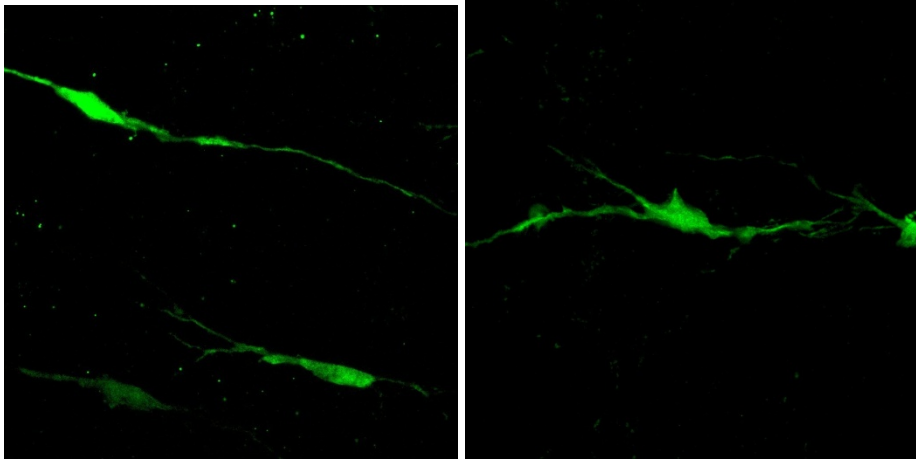

Figure 9.1: *Neuronal generation is observed in the OB of adult mice injected with an EGFP vector (left; control) and with an EGFP vector plus FGS (right). The images show immature neurons having a migratory morphology.*

Work Package 10: Scale-up of CNP-Materials

1. CNP-Membranes
3 CNT variations of a PDMS membrane evaluation pointed out an optimised PDMS / PyrenePOSS-MWCNT system which may present required properties under particular dip coating system settings. Even if feasibility up-scaling has been possible, conductivity has been more difficult to achieve.

2. CNP Bulk composite
Different nanocomposites have been prepared at lab scale and it could be shown that good dispersions of MWCNT in a polyolefin matrix can be achieved by using physisorbed block copolymers, leading to improved mechanical properties. Also the selective incorporation of MWCNT in a two phase polymer blend was achieved. A novel strategy to prepare well-dispersed MWCNT-based nanocomposites is the precipitation polymerisation, where the polymer precipitates and entraps the CNP when a soluble monomer being polymerised.

CNT containing compounds have been produced at pilot scale, based on results from lab scale study. Unfortunately, the promising properties observed at lab scale were not achieved with industrial machines. In the case of high density polyethylene, the percolation threshold is significantly higher than expected despite all process optimisations performed. Therefore, material price is much too high and the solution is not economically viable. Furthermore, dispersing agents like EVA or SEPS are detrimental to fuel barrier performances.

3. CNP-Packaging and foamed materials
Prototypes with rigid PU foam were manufactured by mixing CNT loaded polyol with isocyanate. Properties have been investigated with a particular attention paid to reflectivity. The high conductivity level of labscale experiments with PEG-functionalized CNT's was not achieved after upscaling.

Desired mechanical properties have been reached as prototypes are made with rigid PU foam. Moreover, ULG studied the scaling-up of the CO_2 supercritical foaming of polymer/carbon nanotubes nanocomposites. This investigation revealed problems of processing as CNTs increased melt viscosity and crystallization kinetics of PP when introduced in PP.

Some delays in the initial schedule led industrial partners to readapt some of their tasks. Despite these delays, results have been obtained for each considered applications. These results were not as positive as expected. Thus, considering processing, safety and economical issues, industrialization is not foreseen in the near future.

Work Package 11: Life Cycle Analysis

The results of the simplified LCA especially the environmental impact of MWCNT may be underestimated. This is because of the novelty of CNT containing prototypes and products for which a complete Life-Cycle can only be estimated yet. The important effects are the human and eco toxicological aspects of CNT and the resulting costs for safety issues and dumping. For all of the simulations wastewater treatment but no air cleaning and no waste production was considered, because the basis of the simulations was highly artificial.

As a general advice the use of solvent should either be reduced or a recycling of them should be developed. The solvent could also be replaced by a solvent which is based on renewable sources. Both methods can lead to a reduction of the product costs. Furthermore all estimated production chains should be analyzed again after setting up the prototype plant, in order to identify sensitive process steps for energy savings.

Thus this CED´s are based on the parameters and estimations known from the other work packages. Due to the fact that at the beginning of the LCA only estimations and principal results on the planned processes existed this simplified LCA is only a rough framework for further simulations.

Based on the prices and currently used amounts of CNT in the prototypes the IB members decided that the cost-benefit ratio of CNT filled systems is too low for current applications. But with decreasing international CNT prices methods and processes established within the HARCANA project will get more lucrative compared to the existing systems.